Available online at www.sciencedirect.com
SCIENCE DIRECT®
Journal of Nuclear Materials 348 (2006) 174–180
journal of nuclear materials
www.elsevier.com/locate/jnucmat

Analysis of geometrical effects on graphite oxidation through measurement of internal surface area

Eung Soo Kim *, Kyung Won Lee, Hee Cheon No

Department of Nuclear and Quantum Engineering, Korea Advanced Institute of Science and Technology, 373-1, Guseong-dong, Yuseong-gu, Daejeon 305-701, Republic of Korea

Received 7 July 2005; accepted 16 September 2005

Abstract

To investigate the geometrical effects on nuclear graphite oxidation in the regime where the chemical effect is the rate-controlling process, we introduce the concept of internal surface density into the Arrhenius-type reaction model and suggest how to determine it experimentally. Using the 16 different samples of IG-110 graphite, which have different ratios of external surface to volume, we obtained the value of internal surface density as 17260 m^{-1}. We found out that the external surface reaction is very small compared to the total reaction for the IG-110 graphite: the ratio of the external surface reaction to the total reaction was within 5%. Finally, we propose the following reaction equation for this material:

$$r'''(\mathrm{kg/m^3 s}) \approx 2\,552\,000 \cdot \exp\left(-\frac{218\,000}{R \cdot T}\right) \cdot P_{O_2}^{0.75}.$$

1. Introduction

High temperature gas cooled reactors, which have passive safety features and usefulness for hydrogen production, are expected to become the nuclear reactors of the next generation. At present, the most critical factor in this type of reactor is the problem of air-ingress accident, which is caused by a broken pipe. When air is ingressed into the reactor due to an accident, the graphite materials in the moderator and reflector suffer from a chemical reaction with oxygen. Such a situation would have serious consequences. For instance, the heat generated by exothermic reaction would increase the temperature, the structural integrity would be damaged and the explosive CO gas would accumulate in the reactor. Among the numerous reactions of concern, the most important one is the following graphite oxidation [1]:

$$C + aO_2 \rightarrow bCO + cCO_2 \quad (1)$$

There are many factors affecting the rate of graphite oxidation; temperature, oxygen concentration, moisture, impurities, geometrical factors etc, and

* Corresponding author. Tel.: +82 42 869 3857; fax: +82 42 869 3895.
E-mail address: kes@nsys.kaist.ac.kr (E.S. Kim).

0022-3115/$ - see front matter © 2005 Elsevier B.V. All rights reserved.
doi:10.1016/j.jnucmat.2005.09.018

many researchers [2–11] have obtained many excellent results through investigations. In this study, we are focusing on the geometrical effect, and it is still unsolved part concerned with the graphite oxidation. Generally, graphite has a lot of pores in the inside, so the reaction occurs not only on the external surface but also in the internal pores. The geometrical factor is closely related to the rate of reaction, although it does not affect the original chemical characteristics of the graphite. Therefore, to clearly expand the laboratory scale results to real scale analysis, we need to study the geometrical factors. Previously, Fuller and Okoh [5] investigated the geometrical effects for the nuclear graphite by analyzing the fractal dimension of the porous structure which relates the roughness of internal surface and the interconnectivity of the pore system. They concluded that the nuclear graphite IG-110 is a smooth microporous solid after fabrication. In the present study, we tried to approach this problem more macroscopically and quantified the geometrical effect in the zone I where the chemical reaction is the rate-controlling process.

2. Method of analysis

To investigate the geometrical effect on the graphite oxidation, we developed a new method of analysis. The details are as follows. Since graphite is a porous material, the oxidation reaction occurs not only on the external surface but also in the internal pores, as illustrated in Fig. 1. Therefore, the reaction rate of graphite oxidation (R_g) can be expressed as follows:

$$R_g = A_0 \cdot \exp\left(-\frac{E_a}{R \cdot T}\right) \cdot P_{O_2}^n \cdot (A_s + A_v), \tag{2}$$

where A_0 is a pre-exponent factor, E_a is an activation energy, R is a gas constant, T is the temperature, P_{O_2} is the partial pressure of the oxygen, n is the order of reaction, A_s is the external surface area, and A_v is the internal surface area available for reaction. In order to determine A_v, we assume that A_v is proportional to the volume (V) of the graphite because the internal pores are uniformly distributed:

$$A_v = \theta \cdot V, \tag{3}$$

where θ is an internal surface density, which physically means an internal surface area in unit volume. If we put Eq. (3) into Eq. (2), we can obtain the following equation:

$$\frac{R_g}{A_s} = A_0 \cdot \exp\left(-\frac{E_a}{R \cdot T}\right) \cdot P_{O_2}^n \cdot \left(1 + \frac{\theta \cdot V}{A_s}\right). \tag{4}$$

If the temperature and oxygen pressure are fixed in Eq. (4), the value of $A_0 \cdot \exp(-\frac{E_a}{R \cdot T}) \cdot P_{O_2}^n$ is also fixed. Therefore, we can rewrite Eq. (4) as

$$\frac{R_g}{A_s} = C \cdot \left(1 + \theta \cdot \frac{V}{A_s}\right), \tag{5}$$

where

$$C = A_0 \cdot \exp\left(-\frac{E_a}{R \cdot T}\right) \cdot P_{O_2}^n. \tag{6}$$

In Eq. (5), R_g/A_s is linearly related to V/A_s under constant temperature and oxygen pressure conditions. As illustrated in Fig. 2, $C \cdot \theta$ represents a slope and C represents a y-axis intercept of the linear graph.

In this study, to determine the value of θ, we measured the reaction rates for various graphite samples with different surface-to-volume ratios, and obtained the relation graph shown in Fig. 2. We then calculated θ by analyzing its gradient and y-interception.

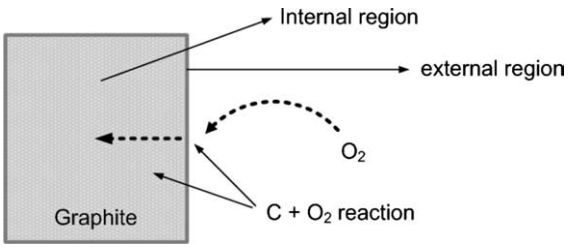

Fig. 1. Schematic of graphite oxidation.

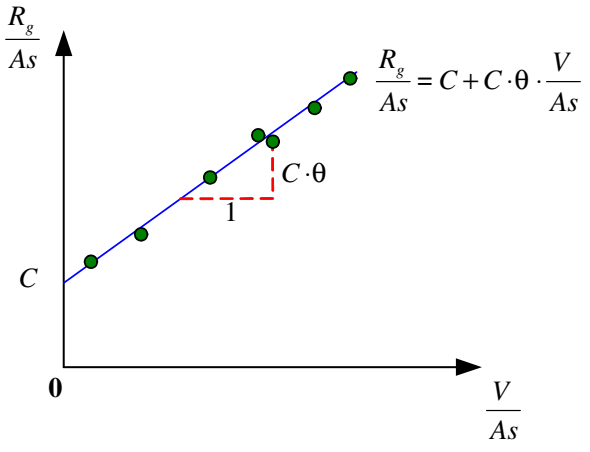

Fig. 2. The trend of R_g/A_s versus V/A_s at a constant temperature and concentration.

3. Experiments

To measure the graphite oxidation velocity, we manufactured the experimental facility, as shown in Fig. 3. We injected dehumidified natural air into the test section through a damping tank, and controlled the flow rate with a mass flow controller within ±1% accuracy. Fig. 4 shows the schematic of the test section, which was made of an electrical furnace. In our experiment, the temperature was constantly maintained at 600 °C within ±1 °C accuracy. The test was carried out under the condition, where the chemical reaction is a rate-controlling process. We placed graphite samples on the beam at the center of the furnace, and connected the support beam to the balance. Weights were measured with a precision of ±1 mg. Internal diameter and length of the furnace were 10 cm and 40 cm, respectively, and air was injected from four ports at the top of the furnace.

We used IG-110 graphite, which is an isostatically molded, isotropic, fine-grained, halogen purified nuclear grade graphite. Table 1 summarizes the properties of this graphite and Fig. 2 summarizes

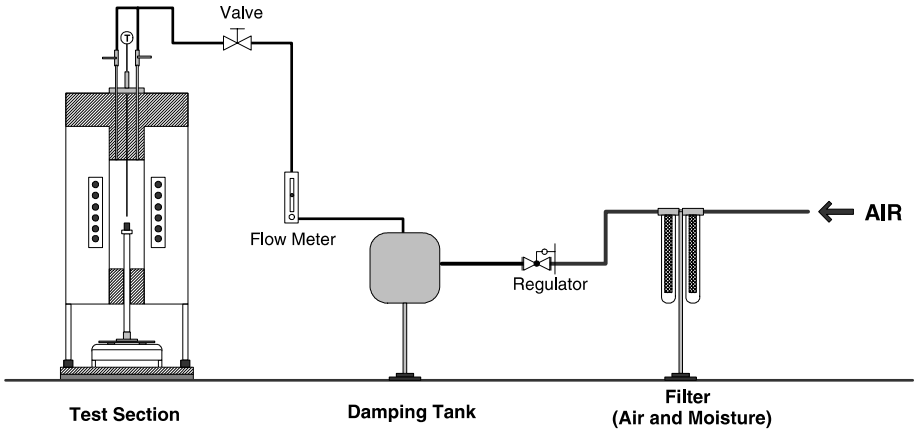

Fig. 3. Schematic diagram of the test facility.

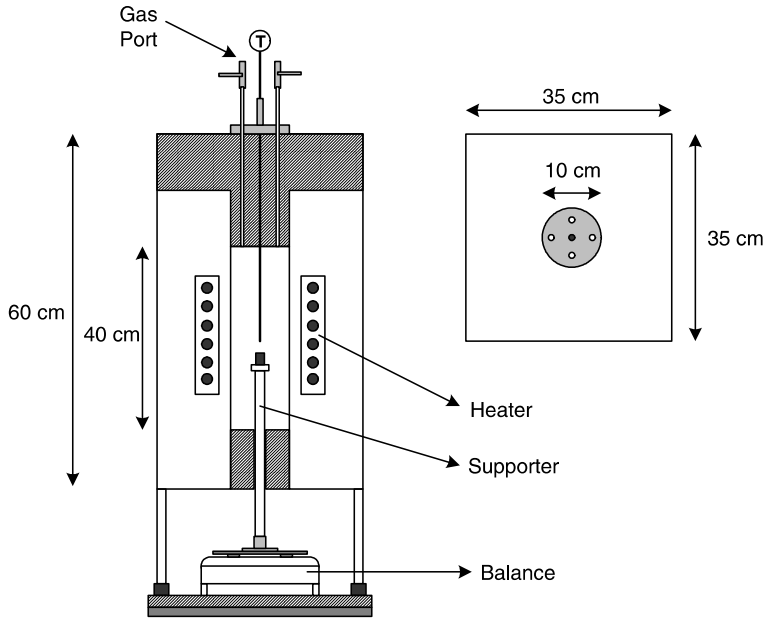

Fig. 4. Test section.

Table 1
Properties of the IG-110 graphite

Material	IG-110
Producer	Toyo Tanso
Bulk density (g/cm^3)	1.75
Young modulus (GPa)	9.6
Compressive strength (MPa)	70.5
Rockwell hardness (MPa)	74.2
Fracture toughness (MPa)	0.82
Thermal conductivity (W/mK)	116
Porosity (vol%)	21.6
Impurities (ppm)	<20

the geometries and sizes of each sample used in our experiment. Fig. 5 illustrates the relative size and geometry of each sample.

4. Results and discussion

In this study, the experiment was performed at 600 °C. Since the reaction is very slow at this temperature, we assumed that the inpore diffusion effect is negligible. To confirm this, we solved the diffusion equation with the oxidation by numerical methods, and obtained the profiles of the reaction rates. Resultantly, the differences between the maximum and minimum values were within 0.7%, which concluded that the inpore diffusion effect was negligible. Our results are only applicable to zone I (low temperature), since the experiment was carried out within zone I.

To obtain the internal surface density, we measured the reaction rates of graphite specimens with different surface-to-volume ratios. Fig. 6 shows one example of the test results. The data were measured for 500 min for the sample number 12 of Table 2. In this graph, the horizontal line represents the time and the vertical line represents the weight of the sample. In this test, only 0.7% of material was consumed by oxidation during 500 min. Totally, 16 types of geometries were tested as summarized in Table 2, and we analyzed them as suggested in Section 2.

As shown in the results of the previous studies [5,9], the rate of graphite oxidation can not be considered as constant in a long time scale because the internal structure of the graphite is highly affected by the oxidation. In this study, we only took the data up to 300 min. Then the maximum weight loss was observed less than 0.7%. This range is a very initial stage of the whole reaction, and it is believed

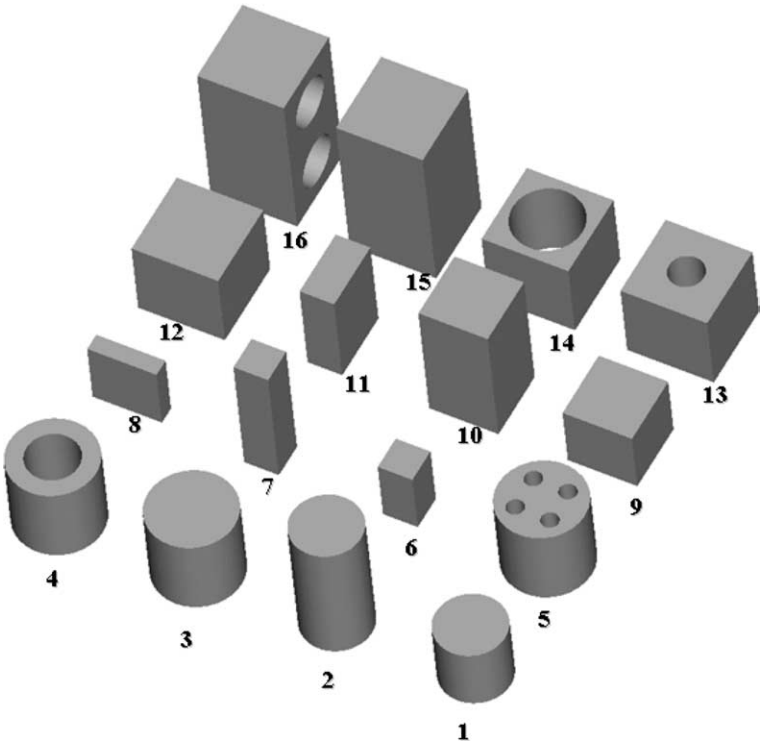

Fig. 5. Relative size and geometry of each sample.

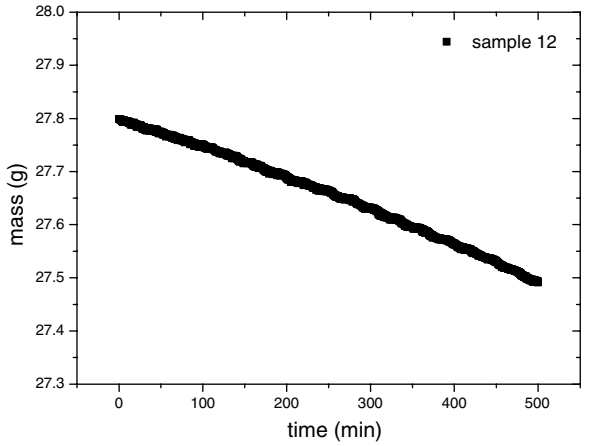

Fig. 6. Experimental results of weight losses of graphite with time (600 °C, sample 12).

that our data will represent the initial geometrical characteristics of the original graphite because no additional porosity was created yet. To estimate the linearity of the mass data, we used statistical analysis and concluded that the reaction rate can be considered as constant within 0.12% error in our time range.

Fig. 7 shows the relation between R/A_s and V/A_s. By analyzing the slope and y-axis intercept of this graph, we deduced the internal surface density as follows:

$$\theta = 12\,760\ \mathrm{m}^{-1}. \tag{7}$$

Physically, it means that a unit volume of graphite includes a 12 760 m^2 internal surface area. With this result, we calculated the proportion (I) of the external surface reaction among the total reaction for each sample. Since the reaction rate is proportional to the surface area, the proportion of external reaction can be calculated by the following equation:

$$I\ (\%) = \frac{A_s}{A_s + A_v} \times 100 = \frac{A_s}{A_s + \theta \cdot V} \times 100, \tag{8}$$

where I (%) means the percentage of the external surface reaction in the total reaction. Fig. 8 illustrates the calculated results: the horizontal and vertical lines represent the number of samples and the percentage of the external surface reaction, respectively. As shown in this figure, the proportion of the external reaction is below 5% of the total reaction, which means that most reactions occur in the internal pore.

Figs. 9 and 10 show the relation between reaction rate and geometrical parameters: volume and surface, respectively. As shown in these figures, the reaction rate shows linear trend to the volume of the graphite, which is strongly related to the internal reaction, while the external surface area does not show any trends. The correlation coefficient between the reaction rate and the volume was calculated as 0.97, and the coefficient for the surface area was 0.85. This result quantitatively shows that the volume is more related variable to the chemical reaction.

On the basis of our experimental results and the previous studies, we determined all parameters in Eq. (4). The chemical parameters E_a and n were selected from previous works on IG-110 graphite

Table 2
Geometry and size of each tested sample

	Type	Size (mm)	Volume (mm^3)	Area (mm^2)	V/A_s (m)
1	Cylinder	D20 × L20	6283	1885	0.0033
2	Cylinder	D20 × L40	12 566	3142	0.0040
3	Cylinder	D25 × L25	12 272	2945	0.0042
4	Cylinder	D25 × L25 (15 mm 1 hole)	7854	3770	0.0021
5	Cylinder	D25 × L25 (5 mm 4 holes)	10 308	4359	0.0024
6	Rectangular	10 × 10 × 20	2000	1000	0.002
7	Rectangular	10 × 10 × 40	4000	1800	0.0022
8	Rectangular	5 × 20 × 20	2000	1200	0.0017
9	Rectangular	20 × 20 × 20	8000	2400	0.0033
10	Rectangular	20 × 20 × 40	16 000	4000	0.004
11	Rectangular	10 × 20 × 30	6000	2200	0.0027
12	Rectangular	25 × 25 × 25	15 625	3750	0.0042
13	Rectangular	25 × 25 × 25 (10 mm 1 hole)	13 662	4278	0.0031
14	Rectangular	25 × 25 × 25 (20 mm 1 hole)	7771	4693	0.0017
15	Rectangular	25 × 25 × 50	31 250	6250	0.005
16	Rectangular	25 × 25 × 50 (15 mm 2 holes)	22 414	7899	0.0028

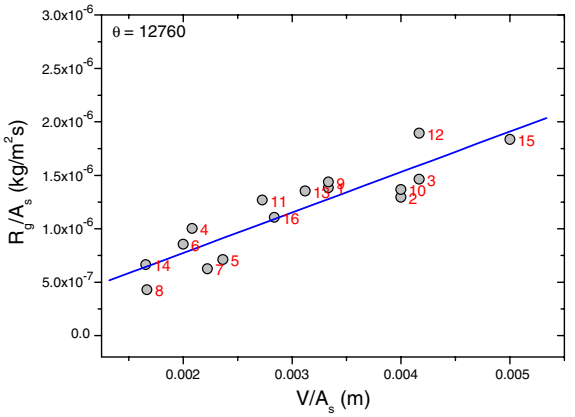

Fig. 7. The results of R_g/A_s versus V/A_s.

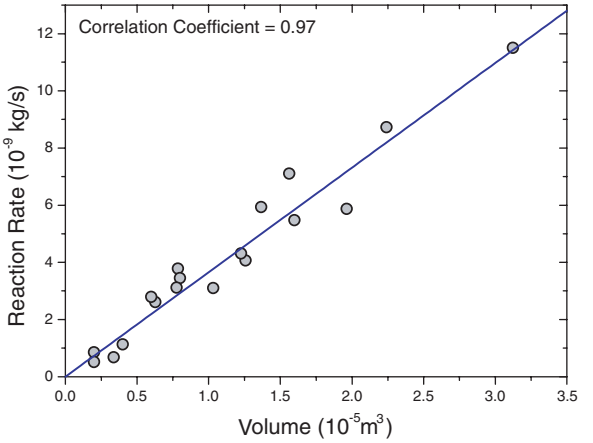

Fig. 9. Relation between the volume and the reaction rate.

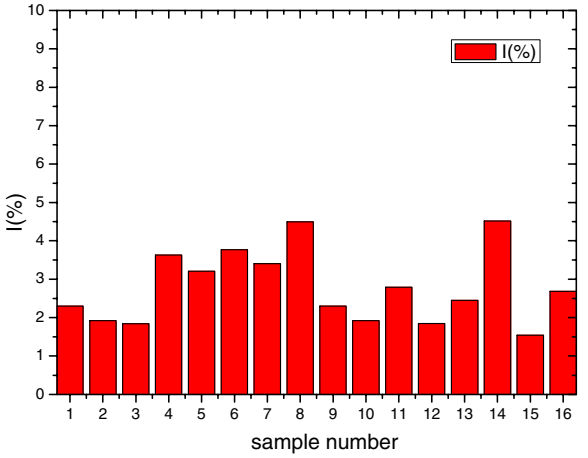

Fig. 8. The portion of the external surface reaction to the total reaction rate.

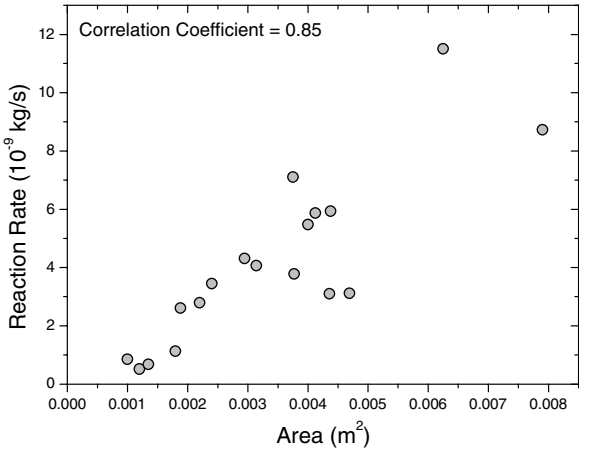

Fig. 10. Relation between the external surface area and the reaction rate.

[5–8,11] and the values were 218 kJ/mol and 0.75, respectively. The value of θ was obtained as 12 760 m^{-1} in the present study. The pre-exponential factor A_0 was obtained as 200 $kg/m^2sPa^{0.75}$ on the basis of our data for the reaction rate. The equation and parameters can be summarized as follows:

$$\frac{R_g}{A_s} = A_0 \cdot \exp\left(-\frac{E_a}{R \cdot T}\right) \cdot P_{O_2}^n \cdot \left(1 + \frac{\theta \cdot V}{A_s}\right), \qquad (4')$$

where

$$A_0 = 200\ (kg/m^2sPa^{0.75}), \quad E_a = 218\ kJ/mol,$$
$$n = 0.75, \quad \theta = 12\,760\ m^{-1}.$$

This equation is applicable for IG-110 graphite when the chemical effect limits the reaction rate. Since the external reaction is negligible, as shown in Fig. 8, we can neglect the terms of the external surface reaction from Eq. (4) as follows:

$$\frac{R_g}{A_s} \approx A_0 \cdot \exp\left(-\frac{E_a}{R \cdot T}\right) \cdot P_{O_2}^n \cdot \theta \cdot \frac{V}{A_s}. \qquad (9)$$

Therefore,

$$R_g \approx A_0 \cdot \exp\left(-\frac{E_a}{R \cdot T}\right) \cdot P_{O_2}^n \cdot \theta \cdot V. \qquad (10)$$

If we rearrange this equation, the final equation is as follows:

$$\frac{R_g}{V} = r'''\ (kg/m^3s) \approx (A_0 \cdot \theta) \cdot \exp\left(-\frac{E_a}{R \cdot T}\right) \cdot P_{O_2}^n, \qquad (11)$$

where r''' represents the volumetric reaction rate.

Since the internal structure of the graphite depends on the degree of burn-off, the Eq. (11) is only applicable to the initial stage of reaction, where no internal structure is changed. However the methodology introduced here can be applied to all of the degrees of burn-off. Since the degree of burn-off tends to increase the internal surface area including the size of the pores, the external surface reaction is expected to be negligible at high burn-off, but more investigations are required.

5. Summary and conclusions

In order to see the geometrical effects of nuclear graphite, we introduced the internal surface density (θ) concept and suggest how to determine it experimentally. Then we suggest the following correlation in the regime where the chemical effect is dominant:

$$r''' \ (\mathrm{kg/m^3 s}) = (A_0 \cdot \theta) \cdot \exp\left(-\frac{E_a}{R \cdot T}\right) \cdot P_{O_2}^n. \quad (12)$$

Using the 16 different samples of IG-110 graphite, we obtained the resultant θ value of $17260\ \mathrm{m^{-1}}$. We found out that the ratio of the external surface reaction to the total reaction was within 5% for the IG-110 graphite. To analyze the effect of the external surface area, we performed the analysis of variance (ANOVA) for the reaction rates normalized by the total surface area and the internal surface area. As a result, since p-value (significance level) was 0.662 and it was much larger than the criteria 0.05, the effect of the external surface area can be considered as negligible. Finally, we suggest the following equation for initial stages of the oxidation for IG-110 graphite:

$$r''' \ (\mathrm{kg/m^3 s}) \approx 2\,552\,000 \cdot \exp\left(-\frac{218\,000}{R \cdot T}\right) \cdot P_{O_2}^{0.75}. \quad (13)$$

Eq. (13) predicts well with our experimental data within 17.8% RMS error.

References

[1] P.L. Walker, F. Rusinko, L.G. Austin, Adv. Catal. 11 (1958) 133.
[2] T. Takeda, M. Hishida, Int. J. Heat Mass Transfer 39 (1996) 527.
[3] H.K. Hinsen, W. Katscher, R. Moorman, KFA, ISSN 0366-0885 (1983).
[4] R. Moorman, S. Alberici, H.K. Hinsen, A.K. Krussenberg, C.H. Wu, In: Proc. of Ninth CIMETC, Florence (1998) 14.
[5] E.L. Fuller, M.J. Okoh, J. Nucl. Mater. 240 (1997) 241.
[6] M. Ogawa, Jpn. Nucl. Soc. 35 (1993) 245.
[7] T. Hino, M. Hashiba, K. Akimoto, T. Yamashina, J Nucl. Sci. Technol. 28 (1991) 20.
[8] H. Kawakami, TANSO 124 (1986) 26.
[9] L. Xiaowei, R.J. Charles, Y. Suyuan, Nucl. Eng. Des. 227 (2004) 273.
[10] M. Takahashi, M. Kotaka, H. Sekimoto, J. Nucl. Sci. Technol. 31 (1994) 1275.
[11] E.S. Kim, H.C. No, NUTHOS-6, Nara, Japan (2004).